Impact of the dielectric duty factor on magnetic resonance in Ag-SiO_2-Ag magnetic absorber*

WANG Yu-ying (王玉颖)[1], **LI Jing** (李晶)[2], **SU Fu-fang** (苏富芳)[1], **SUN Xue-bo** (孙学博)[1], **ZHANG Xu** (张旭)[1], **LI Yan** (李妍)[1], **and ZHANG Xia** (张霞)[1]**

1. Shandong Provincial Key Laboratory of Laser Polarization and Information Technology, School of Physics and Physical Engineering, Qufu Normal University, Qufu 273100, China

2. Surface Physics State Laboratory and Department of Physics, Fudan University, Shanghai 200433, China

(Received 24 November 2019; Revised 17 February 2020)

Magnetic absorber in optical frequency can be fulfilled through metamaterials designing. Therein, magnetic resonance in metal-dielectric-metal metasurfaces can be manipulated conveniently, and studying the parameters impacts is the primary for applications. In this work, through changing the grating width and the thickness of silica, the magnetic resonance modes have been studied, the conditions of the phase change zone from magnetic resonance (MR) to Fabry-Pérot (FP) are given out in Ag-SiO_2-Ag grating magnetic metasurfaces. The results indicate that the MR mode in metal-dielectric-metal configuration is mainly decided on the dielectric duty factor other than the sole behaviors of the thickness of dielectric and size of nanostructures. The physical mechanism is elucidated through simulated electromagnetic field distributions using finite difference time domain (FDTD) solution, and numerical analysis of effective refraction index of Ag-SiO_2-Ag magnetic metasurfaces. This study may prompt development of metamaterials in basic research in condensed physics and in optical devices applications.

Document code: A **Article ID:** 1673-1905(2021)01-0005-7

DOI https://doi.org/10.1007/s11801-021-9200-z

Based on Kirchhoff's law, optical absorber plays important role in photoelectronic setups[1-3]. And metamaterials, which can manipulate light-matter interaction through both magnetic and electronic response, make complete absorber available[4-6]. As well known, magnetic response of natural materials to electromagnetic waves can hardly be realized at optical frequency. But through metamaterials, both the permittivity ε and permeability μ can be designed arbitrarily[7], which facilitate the photoelectronic devices fabrication based on optical absorber[8-10].

To manipulate the magnetic response to the electromagnetic waves in optical frequency, diversity nanostructures have been designed since the negative refraction phenomena proposed by by Veselago in 1969[11]. Using man-made split ring, Pendry firstly experimentally realized manipulating magnetic response in 1999[12]. Since then, magnetic resonance has been studied intensively through diverse optical metamaterials (MM)[13], for example, metallic nanoholes[14], split-ring[15], oligomers[16], high- index nanospheres[17,18], all-dielectric chiral nanostructures[19,20], and metal-dielectric-metal configurations[21], etc. Many novelty phenomena in condensed physics, such as Fano resonance, electromagnetic induced transparency (EIT), and Rabii splitting, PT symmetry (exceptional point) have been studied through the modes coupling in magnetic metamaterials[22-25]. It provides a flexible material platform in sophisticated optical devices design[5-7].

Among multiple resonant unit cell of magnetic absorbers, metal/dielectric/metal (MDM) configuration is a rich plasmonics playground supporting several optical modes. Under the excitation, electrons oscillate at the metal-dielectric interface, and so-called surface plasma plasmons (SPPs) occur at both the up and down metal-dielectric interface of MDM unit cell, where the electron oscillation at the up and down metal-dielectric interface[21,26]. When the electrons oscillation is out-of-phase, namely, the spatial distributions of oscillated electrons are in the antisymmetric attitude, one electronic current nanoloop formed, correspondingly, the magnetic field is augmented according to Lenz's law and magnetic resonance mode occur. Whereas, other optical modes occur when the electrons oscillations are in phase. Magnetic resonance (MR) mode[21,26,27] possesses peculiarities as strongly localize electromagnetic field in the

* This work has been supported by the Natural Science Foundation of Shandong Province (No.2015ZRB019MD), the National Science Fund for Young Scholars (No.11704219), the Doctoral Research Started Funding of Qufu Normal University (No.BSQD20130152), the Open Subject of Key Laboratory of Magnetism and Magnetic Materials, Ministry of Education, Lanzhou University (No.LZUMMM2019013).

** E-mail: xzhangqf@mail.qfnu.edu.cn

dielectric, is commodiously manipulated, and facilitates coupling with other optical modes. And the potential usage had been reported in magnetic nano-laser[28], perfect absorber[29,30], nonlinear generations[31], negative optical pressure[32] and polarization devices[33], etc. In metasurfaces with MDM unit cell periodically patterned, besides the magnetic resonance mode, surface lattice resonances (SLR) occur due to the Bragg scattering[34]. Fano resonance had been studied in periodical MDM systems through the coupling between MR and SLR[35], the prominent features as narrow and asymmetric line shape had been revealed. The coupling between MR and SiO_2 phonon had been studied in Ag-SiO_2-Ag grating systems, through changing the width of Al grating on top of SiO_2 , the first order MRs were modulated, and strong coupling occurred where anticrossing behaviours were presented at wavelength near λ=12.5 μm[36].

Hereby, manipulating magnetic resonance and coupling with other optical modes in MDM magnetic metasurfaces are important in both physical phenomena and application study. For this, the prime work is studying the parameters impact on optical modes in MDM metasurfaces, which has been reported that MR is insensitive to the size, the form of lattice and the thickness of the dielectric spacer[37]. Therein, the dielectric spacer plays the key roles in manipulating MR, as analysed above, the MR optical mode comes from the current nano-loop formed in the near field due to the anti-parallel surface currents in the up and down metal-dielectric interface. When the spacer layer is too thick, the current nano-loop cannot come into being, and thus no MR occurs. As well known, optical mode of Fabry-Pérot (FP) cavity can occur in optical film of metal-insulator-metal Bragg reflector once meeting the half wave condition. Chen group studied the transmission/reflection characteristics of a periodical MDM system with thick dielectric spacer using multiple-scattering method, and found perfect absorbers occurred due to the interference effect[38]. Using one-dimensional metal grating covered on insulator/metal film, the near-field coupling were studied in microwave region, and the phase change condition between MR and FP was analytically given out[39]. The distribution laws of electric field and magnetic field for MR and FP optical modes in MDM configuration are not the same. For MR, the electromagnetic (EM) fields are mainly distributed in the insulator, whereas for FP modes, the EM field are distributed both in free space and the insulator. Most physical characteristics come from these different EM field distributions law of optical modes.

Although the thickness of dielectric layer is the key factor in MR mode occurring, it is not the only decisive parameter. In this paper, through analysing the MR modes in Ag-SiO_2-Ag magnetic MTS with Ag grating arrayed on the SiO_2/Ag film, the duty factor impact of dielectric lay SiO_2 are studied. The physical mechanism is elucidated through simulated electromagnetic field distributions using finite difference time domain (FDTD) solution, and numerical analysis of effective refraction index. The simulation of all the spectra and EM field distribution are performed using commercial software FDTD solution (Lumerical Solutions Colt.) based on finite difference time domain method. In simulation, the optical parameter of Ag comes from the data base of FDTD solution software, and the dielectric SiO_2 is measured using ellipsometry (JOBIN YVON, UVISEL) and fitted by Lorentz-Drude model. An adaptive mesh of 1 nm is used to precisely model the shape of the nanostructures.

The schematic plot of Ag-SiO_2-Ag configuration is presented in Fig.1(a). Firstly, the silver film of thickness t=150 nm was deposited on silicon substrate, and Ag film was thick enough to prohibit light transmission. Amorphous silica films with thickness d was synthesized on Ag film, which acted as dielectric layer. The optical properties of silica in the data base of software FDTD solution are in accordance with the silica synthesized by PECVD at temperature 300 ℃ on the Al film, as can be referred to our experimental work[40]. To demonstrate parameters impact on the optical modes in metal-dielectric-metal system, the simple nanostructure with one-dimensional (1D) Ag grating structure on uppermost layer is used in the study, where the height of grating is h=0.05 μm. The other parameters, such as the period Λ, width b, and thickness of the dielectric layer as denoted in Fig.1(a) are all objects of study, and a general conclusion about the impacts of these parameters on reflectivity would be drawn.

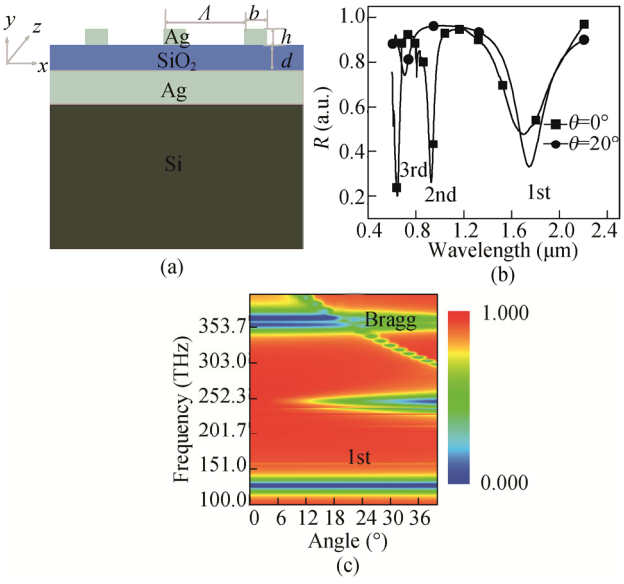

Fig.1 (a) The schematic plot of MDM structures; (b) The reflection spectra under the incident angles of θ=0° and θ=20°; (c) Angle-resolved reflection spectrum of samples with Λ=0.6 μm, b=0.3 μm, d=0.03 μm and h=0.05 μm

To ravel optical modes in Ag-SiO_2-Ag magnetic metasurfaces[41], angle-resolved reflection spectra of sample with grating period Λ=0.6 μm, width b=0.3 μm, and the thickness of silica d=0.03 μm are given out in Fig.1(b) and (c). Firstly, the reflection spectra versus wavelength with incident angle θ=0° (normal incident) and θ=20° are presented in Fig.1(b), for clarity, the dips are marked out. Compared with reflection spectrum at θ=0°, dip 1st in reflection spectrum at θ=20°becomes shallower and is red-shifted slightly. Dip 3rd is deeper at θ=20° than that at θ=0°. Furthermore, the Bragg mode occur with varying incident angle, which overlap with dip 2nd, as can be seen in Fig.1(b). Besides dips 1st and 2nd, one prominent dip locate at λ=0.93 μm is demonstrated in reflection spectrum at θ=20°, which have not been found in reflection spectrum at incident angle θ=0°, and we deduce that it is sub-radiation mode according to Ref.[42]. The evolution of these optical modes with incident angle can be revealed through the contour plot analysis in Fig.1(c). As can be seen, dips 1st and 3rd remain unchanged with incident angle, the gradually degraded intensity of dip 3rd might come from the overlapping with Bragg mode, which red-shift with the increment of incident angle. Dip 2nd gradually become intensive with increasing incident angle, which is no radiation at low-angle, and can be ascribed to dark mode. Both bright modes corresponding to dips 1st and 3rd and dark mode corresponding to 2nd are all localized states, where the location are remain unchanged, whereas that of Bragg mode is red-shifted with increasing the incident angle. Here, for the thin thickness of dielectric layer (compared with study wavelength), the localized optical modes corresponding to 1st, 2nd, and 3rd dips, are ascribed to 1st, 2nd, and 3rd magnetic resonance (MR) modes, respectively.

The dependence of optical modes as function of wavelength on parameters as periodicity Λ (a), grating width b (b), and thickness of silica dielectric d (c, d) are illustrated in Fig.2. As can be seen in Fig.2(a), when fix the width of grating b=0.3 μm and the thickness of silica d=0.03 μm, then change the lattice from 0.5 μm to 1 μm, two narrow oblique lines (the dark green line) varying with the lattice can be discerned, they might come from the surface wave diffracted by the periodic structure, because they are sensitive to changes of the lattice, and can be attributed to 1st and 2nd order surface lattice resonance (SLR) are marked out by the dark green line. The location of the SLR are as linear function of lattice in this one dimensional grating nanostructure. Besides, one vertical broad line locate near λ=1.7 μm and a narrow one locate near λ=0.6 μm can be seen in Fig.2(a) (the purple dashed line), which do not change with the lattice Λ. Compared with those in Fig.1(b) and (c), we can identify them as 1st and 3rd magnetic resonance modes. With fixing the lattice Λ=0.6 μm and the thickness of silica d=0.03 μm, these two localized modes (the white vertical bar) vary when changing the width b from 0.1 μm to 0.4 μm, as can be seen in Fig.2(b) the purple dashed line, the blue vertical bar indicated the location of the two localized mode in Fig.2(a). These two localized modes are sensitive to the geometry of nanostructure, and can be further attributed to 1st (λ≈1.7 μm) and 3rd (λ=0.6 μm) magnetic resonance mode, respectively. In Fig.2(b), one vertical narrow line locate at wavelength λ=0.6 μm, which is near to that of lattice Λ, and can be further consolidated as 1st SLR mode.

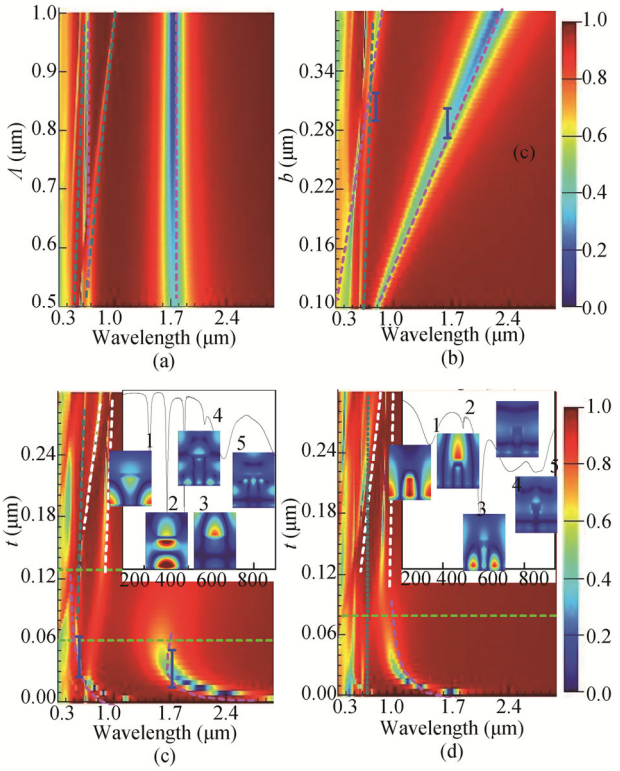

Fig.2 The optical mode in MDM dependence on parameters of (a) the lattice, (b) the radius, and (c,d) the thickness of silica

As analyzed above, magnetic resonance comes from the circumflux formed by the antiparallel SPP waves at the up and down dielectric-metal interface, the energy of MR is located in the dielectric, so magnetic resonance mode is sensitive to the properties of the dielectric layer. Fig.2(c) give out the optical modes dependence on the thickness of space layer silica, where the lattice is fixed at Λ=0.6 μm and the width of grating b=0.3 μm, the thickness of silica d changes from 0 to 0.3 μm. As indicated by the dashed dark green line in Fig.2(c), the SLR hardly vary with changing the thickness of silica. The MR modes in Fig.2(a) (dashed purple line) are marked out by the blue vertical bar in Fig.2(c). Clearly, both 1st and 3rd MR are blue shifted and weakened with the space layer thickening as indicated by the dashed purple curve in Fig.2(c), and these MR modes become weaker and weaker in the zone from d≈0.08—0.15 μm. At the same time, two principal modes occur and become stronger and vary linearly with the thickness of space

layer, as marked by the dashed white line in Fig.2(c). Especially, the location wavelength is enormously blue-shifted, and the intensity becomes stronger with the dielectric layer further thickening. To clarify the physical mechanism of these modes, the reflections of sample with d=0.22 μm as function of frequency in the unit of THz are presented in the interpolated plot in Fig.2(c), along with which are magnetic field distribution corresponding to five dips. Clearly, the dips in reflection spectrum are well-distributed with frequency interval Δv=88 THz, and the corresponded magnetic field distribution are all demonstrating interference pattern both in the dielectric and the free space. According to the dielectric dependence study at the microwave frequency by Lei Zhou group[39], we can deduce that modes changing from magnetic resonance to FP resonance occur in Ag-SiO_2-Ag sandwiched system with dielectric layer thickening. We name the thickness interval denoted by the dashed light green line in Fig.2(c) as phase change zone. When grating width is b=0.15 μm, this phase change zone become as narrow as one line, as can be seen in Fig.2(d) the dashed light green line, and the MR (dashed purple line) and FP (dashed white line) can hardly be discerned at the phase change zone. The reflection spectrum near the phase change zone with d=0.18 μm and corresponded magnetic field distribution of dips are presented in the interpolated plot in Fig.2(d). As can be seen, the diffraction pattern occurs in magnetic field distribution of dips 4 and 5 in high frequency region. The wavelength location of dip 2 in Fig.2(d) and dip 3 in Fig.2(c) are near period of samples, which demonstrate the surface lattice mode peculiarities for that the magnetic field of these two dips are mainly distributed in free space. However, there are difference between the magnetic field distributions of dip 3 in Fig.2(c) and that of dip 2 in Fig.2(d), with obvious diffraction patterned in the dielectric layer for magnetic field of dip 3 in Fig.2(c), nearly homogenous distribution of that of dip 2 in Fig.2(d). We may attribute them to the hybrid of surface lattice mode with FP and MR modes for dip 3 in Fig.2(c) and dip 2 in Fig.2(d), respectively. The magnetic field distribution of dip 2 in Fig.2(c) demonstrate diffraction pattern both in dielectric and free space, it must come from the FP interference. The magnetic field of dip 1 in Fig.2(c) and dips 1, 3 in Fig.2(d) are mainly localized in silica, and demonstrate MR properties. It can be deduced that whether the MR or FP mode occur in MIM configuration are decided on the duty factor of dielectric layer related to the thickness and width of metal-dielectric-metal sandwich. The impact of duty factor of dielectric layer on MR would be preliminarily studied through EM field distribution analysis below.

As can be seen from Fig.3, the electric field $\boldsymbol{E}_y$ distributed in the dielectric layer become attenuated with the silica thickening from 0.01 to 0.14 (Fig.3(I)—(IV)) for samples with varying width b, which is corresponding to the results in Fig.2(c). When the thickness of silica d≈0.14 (IV) in the phase change zone indicated in Fig. 2(c) the dashed bright green line, the field $\boldsymbol{E}_y$ localized in silica is hardly discerned. However, with varying width b=0.15 μm, 0.3 μm and 0.45 μm in Fig.3, the field $\boldsymbol{E}_y$ of 1st MR localized in the dielectric layer become strengthened, and weakened at the up metal-dielectric interface and free space.

The corresponded amplitude distribution of magnetic field $|H_z|$ are presented in Fig.4. It is obvious that one stubs localized in the dielectric layer occur in the magnetic field distribution $|H_z|$ in Fig.4 for all samples, which meet with Lenz' law as analyzed above. With the silica thickening from 0.01 μm to 0.14 μm, the magnetic field $|H_z|$ distributed in the dielectric layer also become attenuated as that of electric field $\boldsymbol{E}_y$ in Fig.3. Furthermore, the field $|H_z|$ of 1st MR localized in the dielectric layer become strengthened with varying width b=0.15 μm, 0.3 μm and 0.45 μm, as can be seen clearly in Fig.4, especially for samples with the thickness of silica d≈0.14 (Fig.4(IV)) in the phase change zone, the field $|H_z|$ localized in silica is hardly discerned when width b=0.15 μm in Fig.4(d), but that is clearly seen for sample with width b=0.45 μm in Fig.4(n). We may outline that the duty factor of space layer is important for magnetic resonance mode occurring. The intensity and position of MR are linearly proportional to grating width, or to say, are linearly proportional to the effective dimensions of dielectric perpendicular to the wave vector of light, whereas, as for thickness of the dielectric, which is at the dimension parallel to the wave vector, the intensity and position of MR demonstrate complex dependence on it.

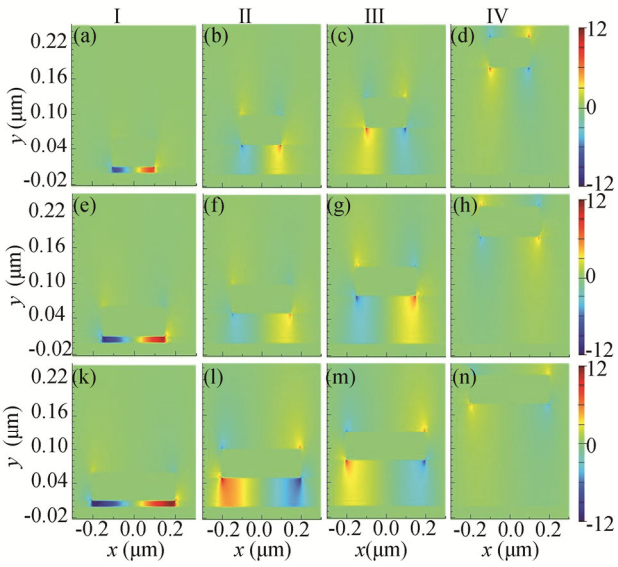

Fig.3 Distributions of field E_y of 1st MR in the *xy*-plane of samples with fixed lattice Λ=0.6 μm, varied width (a-d) b=0.15 μm, (e-h) b=0.3 μm, (k-n) b=0.45 μm, and thickness of silica (I) d= 0.01 μm, (II) d=0.05 μm, (III) d= 0.08 μm, (IV) d=0.14 μm

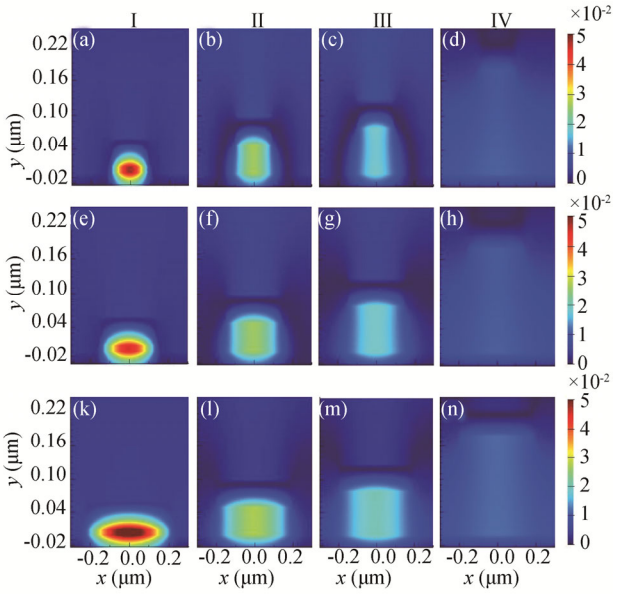

Fig.4 Distributions of field $|H_z|$ of 1st MR in the *xy*-plane of samples with fixed lattice *Λ*=0.6 μm, varied width (a-d) *b*=0.15 μm, (e-h) *b*=0.3 μm, (k-n) *b*=0.45 μm, and thickness of silica (I) *d*= 0.01 μm, (II) *d*=0.05 μm, (III) *d*= 0.08 μm, (IV) *d*=0.14 μm

From above, we define the dielectric duty factor as the ratio of the dimensions parallel and perpendicular to wave vector of light thickness of dielectric, namely d/b. The 1st MR peaks position dependence on duty factor are studied with the peak position of 1st MR normalized to grating width b as λ/b. Fig.5 depicts the simulated (the black line) and fitted (the red line) normalized peak position λ/b spectra versus duty factor d/b. Obviously, the results fitted by function agree that of simulated well, this consolidate the validity of functions we used. As divided by the blue vertical bar in Fig.5, the fitting are performed in two segments. On the left side of the blue vertical bar, the exponential function are used to fit the curve, and on the right, linear function is used. Combined with the result of thickness dependence scanning in Fig.2(c), the location of vertical bar should correspond to phase change zone, where both the weak FP mode and MR coexist, as indicated by the dashed bright green line in Fig.2(c). The phase change zone blue-shifted in d/b axis with increasing the grating width from Fig.5(a)—(g). Furthermore, with increasing grating width from b=0.15 μm (Fig.5(a)) to b=0.45 μm (Fig.5(g)), the exponential curve become steeper, meanwhile, the slope of lines become larger. The fitting formula are outlined in Tab.1, where x is duty factor of SiO_2, and y is the normalized peak position of 1st MR. It can be seen that when the grating width increasing, the absolute value of decaying index in the middle column of the table enhance gradually, at the same time, the slopes of the linear in the right column of the table also be gradually enhanced. All these parameters exhibit rich underlying physics about the optical dependence on the duty factor of the dielectric layer.

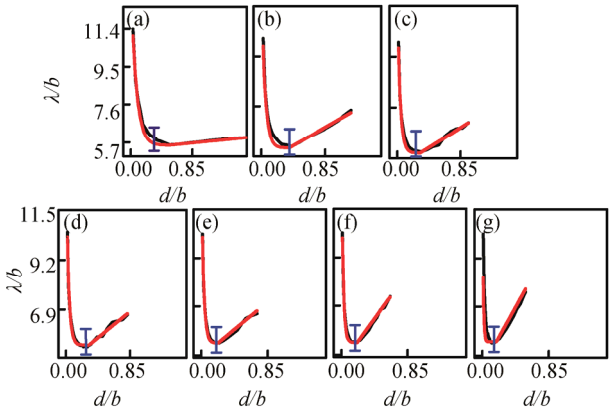

Fig.5 Normalized peaks position versus normalized thickness of silica for samples with (a) *b*=0.15 μm, (b) *b*=0.2 μm, (c) *b*=0.25 μm, (d) *b*=0.3 μm, (e) *b*=0.35 μm, (f) *b*=0.4 μm, and (g) *b*=0.45 μm

For metal-dielectric-metal sandwiched waveguide, when fixed the thickness of dielectric layer, the equation of effective refractive index of transverse magnetic mode was given in Collin's work[43] as follows:

$$n_{\text{eff}} = \frac{k}{k_0} = \sqrt{\varepsilon_{\text{d}}}\left(1 + \frac{\lambda}{\pi b\sqrt{-\varepsilon_{\text{m}}}}\sqrt{1 + \frac{\varepsilon_{\text{d}}}{-\varepsilon_{\text{m}}}}\right)^{1/2}, \tag{1}$$

where ε_{m} and ε_{d} are the permittivity of metal and dielectric layer, and b is the width of the patch, and λ is the resonant wavelength of optical modes. In case of optical modes analyzed in this work, the duty factor d/b play vital role on MR modes with wavelength position normalized to width b as λ/b. Therefore, Eq.(1) can be improved as

$$n_{\text{eff}} = \sqrt{\varepsilon_{\text{d}}}\left(1 + \frac{y}{\pi\sqrt{-\varepsilon_{\text{m}}}}\sqrt{1 + \frac{\varepsilon_{\text{d}}}{-\varepsilon_{\text{m}}}}\right)^{1/2}, \tag{2}$$

where $y=\lambda/b$, and the expressions of y are defined as that in Tab.1.

Tab.1 The functional relationship of magnetic resonance with dielectric thickness with different gratings

Width	Exponential fitting	Linear fitting
b=0.15 μm	$y=8.75e^{-14x}+5.81$	$y=0.37x+5.36$
b=0.2 μm	$y=8.77e^{-25x}+5.64$	$y=2.23x+4.55$
b=0.25 μm	$y=9.01e^{-33x}+5.41$	$y=2.64x+4.41$
b=0.3 μm	$y=8.66e^{-38x}+5.27$	$y=2.75x+4.59$
b=0.35 μm	$y=8.64e^{-50x}+5.24$	$y=3.21x+4.37$
b=0.4 μm	$y=9.08e^{-50x}+5.29$	$y=5.55x+3.85$
b=0.45 μm	$y=9.66e^{-62x}+5.41$	$y=7.25x+3.55$

Based on Eq.(2), the effective refractive index of magnetic metasurfaces with varied grating width were numerically calculated. Fig.6 displays calculated effective refraction index versus duty factor d/b for samples with different width. With increasing the duty factor of die-

lectric, the effective refractive index of all samples with different width firstly drops abruptly, and then vary slowly, at last, it tends to one fixed value. Furthermore, it becomes smaller with increasing the grating width from b=0.15 μm to b=0.45 μm in Fig.6, and finally it approach the refraction index of silica n≈1.4 for samples with larger grating width.

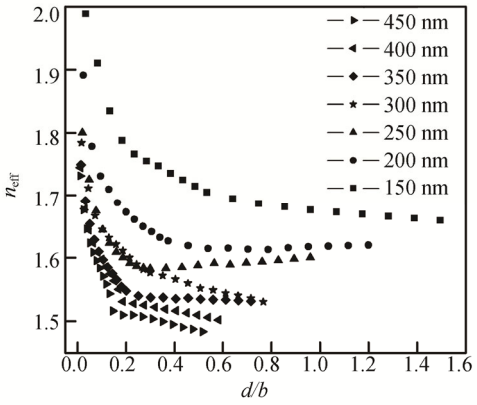

Fig.6 The effective refractive index as a function of duty factor for samples with different widths

In conclusion, the parameters impact on magnetic resonance in periodical Ag-SiO_2-Ag grating magnetic metasurfaces were theoretically studied. By analyzing the shift of the 1st MR position in reflection spectra with varied grating width and the thickness of SiO_2, we found that whether the occurrence of MR or FP mode in MDM configuration are decided not solely on dielectric thickness or size of up metal patches. The dielectric duty factor related to both the dielectric thickness and the size of the up metal patches play vital role on magnetic resonance. The phase changing and the dependence law on duty factor were outlined through electromagnetic field distribution analysis and data fitting. Finally, the effective refraction index of periodical Ag-SiO_2-Ag grating magnetic metasurfaces are numerically calculated, and the physical mechanism are elucidated. This work may prompt the application of magnetic resonance modes in condensed physics phenomena study and optical device designing.

References

[1] Lagatsky A A, Kisel V E, Bain F, Brown C T A, Kuleshov N V and Sibbett W, Advances in Femtosecond Lasers Having Enhanced Efficiencies, International Conference on Lasers, Applications, and Technologies: Advanced Lasers and Systems, 67310E (2007).

[2] Bellaidi A, Ernst K and Könenkamp R, MRS Proceedings **822**, S7.5 (2004).

[3] Wu D, Liu Y, Li R, Chen L, Ma R, Liu C and Ye H, Nanoscale Research Letters **11**, 483 (2016).

[4] Hao J, Wang J, Liu X, Padille W J, Zhou L and Qiu M, Applied Physics Letters **96**, 4184 (2010).

[5] Wang Y, Sun T, Paudel T, Zhang Y, Ren Z and Kempa K, Nano Letters **12**, 440 (2012).

[6] Chen X Wu, J H, Liu C and Cao P, Journal of the Optical Society of America B **36**, 153 (2019).

[7] Zhang X, Optical Metamaterials, London: Springer-Verlag GmbH, 207 (2010).

[8] Longhi S, Physical Review A **82**, 031801 (2010).

[9] Zhang X, Fan Y, Qi L and Li H, Optical Materials Express **6**, 2448 (2016).

[10] Caligiuri V, Palei M, Imran M, Mana L and Krahne R, ACS Photonics **5**, 2287 (2018).

[11] Viktor G Veselago, Soviet Physics Uspekhi **10**, 509 (1968).

[12] Pendry J B, Holden A J, Robbins D J and Stewart W J, IEEE Transactions on Microwave Theory and Techniques **47**, 2075 (1999).

[13] Monticone F and Alu A, Journal of Materials Chemistry C **2**, 9059 (2014).

[14] H W Kihm, S M Koo, Q H Kim, K Bao, J E Kihm, W S Bak, S H Eah1, C Lienau, H Kim, P Nordlander, N J Halas, N K Park and D S Kim, Nature Communications **2**, 451 (2011).

[15] Lahiri B, McMeekin Scott G, Khokhar Ali Z, De La Rue Richard M and Johnson Nigel P, Optics Express **18**, 3210 (2010).

[16] Hentschel M, Saliba M, Vogelgesang R, Giessen H, Alivisatos A P and Liu N, Nano Letters **10**, 2721 (2010).

[17] Fu Y H, Kuznetsov A I, Miroshnichenko A E, Yu Y F and Luk'yanchuk B, Nature Communications **4**, 1527 (2013).

[18] Liu W, Andrey E M and Yuri K, Chinese Physics B **23**, 047806 (2014).

[19] Paweł Woźniak, Israel De Leon, Katja Höflich, Caspar Haverkamp, Silke Christiansen, Gerd Leuchs, and Peter Banzer, Optics Express **26**, 19275 (2018).

[20] Jahani S and Jacob Z, Nature Nanotechnology **11**, 23 (2016).

[21] Lu D Y, Liu H, Li T, Wang S M, Wang F M, Zhu S N and Zhang X, Physical Review B **77**, 214302 (2008).

[22] Wu C, Arju N, Kelp G, Fan J A, Dominguez J, Gonzales E, Tutuc E, Brener I and Shvets G, Nature Communications **5**, 3892 (2014).

[23] Yang Y, Kravchenko I I, Briggs D P and Jason Valentine, Nature Communications **5**, 5753 (2014).

[24] Parinda Vasa, Wei Wang, Robert Pomraenke, Melanie Lammers, Margherita Maiuri, Christian Manzoni, Giulio Cerullo, and Christoph Lienau, Nature Photonics **7**, 128 (2013).

[25] Alaeian H and Dionne J A, Physical Review B **91**, 245108 (2015).

[26] Bo Zhen, Chia Wei Hsu, Yuichi Igarashi, Ling Lu, Ido Kaminer, Adi Pick, Song-Liang Chua, John D. Joannopoulos and Marin Soljačić, Nature **525,** 354 (2015).

[27] Chen H, Luo Y, Liang C, Li Z, Liu S and Lin A, Journal of Optics **20**, 035102 (2018).

[28] Tsurimaki Y, Tong J K, Boriskin V N, Semenov A, Ayzatsky M I, Machekhin Yuri P, Chen G and

Boriskina S V, ACS Photonics **5**, 929 (2018).
[29] Hao J, Jing W, Liu X, Willie J Padilla Zhou L and Qiu M, Applied Physics Letters **96**, 4184 (2010).
[30] Liu N, Mesch M, Weiss T, Mario H and Harald G, Nano Letters **10**, 2342 (2010).
[31] Liu H, Li G X, Li K F, Chen S M, Zhu S N, Chan C T and Cheah K W, Physical Review B Condensed Matter **84**, 2461 (2012).
[32] Liu H, Jack N, Wang S B, Lin Z F, Hang Z H, Chan C T and Zhu S N, Physical Review Letters **106**, 087401 (2011).
[33] Bao Yanjun, Zhu Xing and Fang Zheyu, Scientific Reports **5**, 11793 (2015).
[34] Tserkezis C, Papanikolaou N, Gantzounis G and Nikolaos Stefanou, Physical Review B **78**, 165114 (2008).
[35] R Nicolas, G Lévêque, J Marae-Djouda, G Montay, Y Madi, J Plain, Z Herro, M Kazan, P Adam and T Maurer, Scientific Reports **5**, 14419 (2015).
[36] Zhang X, Liu H, Zhang Z G and Wang Q, Scientific Reports **7**, 41858 (2017).
[37] Yiting C, Jin D and Min Y, Optics Express **22**, 30807 (2014).
[38] Chen H T, Optics Express **20**, 7165 (2012).
[39] Ma S, Xiao S and Zhou L, Physical Review B **93**, 045305 (2016).
[40] H. Liu, Y M L, T Li, S M Wang, S N Zhu and X Zhang. Magnetic Plasmon Modes Introduced by the Coupling Effect in Metamaterials, 247 (2010).
[41] Shi L, Hakala T K, Rekola H T, Martikainen J P, Moerland R J and Törmä P, Physical Review Letters **112**, 153002 (2014).
[42] Lee B J, Wang L P and Zhang Z M, Optics Express **16**, 11328 (2008).
[43] Collin S, Pardo F and Pelouard J L, Optics Express **15**, 4310 (2007).